ACES Asian Chemical Editorial Society

doi.org/10.1002/asia.202400340

CHEMISTRY AN ASIAN JOURNAL Research Article

www.chemasianj.org

Effect of the Imidazole π-Extension on TADF Emitters in Electrochemiluminescence

Elisa Pelorosso,[a] Giulio Pavan,[a] Thomas Scattolin,[a] Laura Orian,[a] Sabrina Antonello,[a] Nicola Demitri,[b] and Alessandro Aliprandi*[a]

Already known molecules which exhibit good electrochemiluminescence (ECL) efficiencies and high photoluminescence quantum yields (PLQY) have been structurally modified in order to increase their performance. The followed strategy is to stiffen the structures to limit the rotational and vibrational freedom degrees and favour radiative decay processes once excited. Molecules under investigation consist of donor-acceptor systems in which the acceptor fraction is a benzonitrile with an imidazole in *para* position, while the donor fraction consists of four diphenylamine (NPh_2) or 3,6-di(*tert*-butyl)-9*H*-carbazole ($^{t\text{-}Bu}Cz$) groups in the remaining positions on the central benzene ring. Therefore, in order to stiffen these systems and restrict the intramolecular rotations (RIR), the imidazole in the *para* position has been replaced with more extended π-systems, i.e., benzimidazole and phenanthro[9,10-d]imidazole. The restriction of the intramolecular rotation can be clearly observed by ^{1}H NMR analysis. We expected to observe an increase in ECL efficiency and PLQY with the rigidity. Surprisingly, we observed a generally opposite trend: molecules with the smallest imidazole fraction showed the best performance in ECL and higher PLQY. Notably, NPh_2 derivatives with benzimidazole and phenanthro[9,10-d]imidazole showed an hypsochromic shift of the emission spectra with concomitant increase of the PLQY as the solvent polarity increases.

Introduction

Thermally activated delayed fluorescence (TADF) emitters have gained increasing appeal as an alternative to heavy metal phosphorescent transition metal complexes (TMCs) in several fields: from organic light emitting diodes (OLEDs)[1,2] to photocatalysis[3] and, more recently, to electrochemiluminescence (ECL).[4] Such compounds are organic molecules that, by a judicious molecular design,[5,6] display extremely small singlet–triplet energy gap (ΔE_{ST}) that allows an efficient endothermic reverse intersystem crossing (RISC) at room temperature.[4,7] This enables excited triplet states to contribute to the fluorophore emission when excitons are produced through nonradiative chemical or electrochemical processes, such as by charge recombination process, as in the case of OLEDs and in electrochemiluminescence.[4,8] Electrochemiluminescence (ECL) is an eye-catching and versatile phenomenon that exploits electrochemical spatio-temporal control to produce excited states capable of emitting light. This intriguing interdisciplinary field has gained significant attention for its application in analytical chemistry, biosensors, and materials science. One of the remarkable features of ECL is its sensitivity and selectivity, making it a powerful tool for analytical techniques such immunoassays. Additionally, ECL has found applications in the development of biosensors, where the specificity of biological recognition elements combines with the sensitivity of ECL to enable rapid and precise detection of various analytes.[9] At its core, ECL involves the generation of excited states through electrochemical reactions, leading to the subsequent emission of light.[10,11] Recently, TADF emitters have proven to be a valid alternative to phosphorescent metal complexes showing high efficiencies.[4] More generally, the ECL efficiency of an emitter depends not only on the ability to capture the triplet excited states, but also on the photoluminescence quantum yield (PLQY) and, above all, on the stability of the transient radical species formed during the electrochemical process.[12] In one of our recent contributions, we have reported a series of TADF emitters constituted by 4-(1H-imidazol-1-yl)benzonitrile as acceptor with different donor moieties (e.g. carbazole and diphenylamine derivatives) showed in Figure 1 (BnIm derivatives).[13]

Our objective was to establish correlations between the photophysical and electrochemical properties of these compounds and their performance in electrochemiluminescence (ECL) using benzoyl peroxide as a co-reactant. Remarkably, some compounds exhibited ECL efficiencies surpassing the standard $[Ru(bpy)_3]Cl_2$ by a remarkable factor of up to 28 times. Interestingly, the imidazole moiety within the compounds can be conveniently alkylated, providing an avenue for the incorporation of functional groups such as carboxylic acid. This functionalization broadens the practical applications of the compounds, showing their potential versatility in

[a] E. Pelorosso, G. Pavan, T. Scattolin, L. Orian, S. Antonello, A. Aliprandi
Dipartimento di Scienze Chimiche, Università degli studi di Padova,
Via Marzolo 1, 35131 Padova, Italy
E-mail: alessandro.aliprandi@unipd.it

[b] N. Demitri
Elettra-Sincrotrone Trieste, S.C.p.A, 34149 Basovizza, Trieste, Italy

Supporting information for this article is available on the WWW under https://doi.org/10.1002/asia.202400340

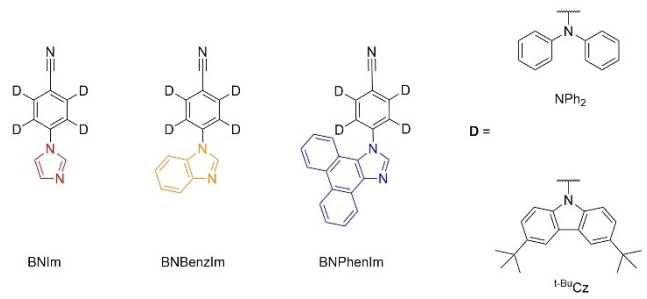

Figure 1. Structures of investigated TADF compounds.

various contexts. However, it significantly reduces their ECL efficiency which drops to one sixth of the corresponding non-alkylated compound.

It is reported that densely combining donors and acceptors as well as strengthening the rigidity of the molecular structure can enhance the radiative luminescence efficiency.[14] Indeed, the restriction of the intramolecular rotation (RIR) is a well-known phenomenon that lead to the aggregation induced emission (AIE) phenomenon in the solid state.[15] Therefore, together with the aim of further investigating the role of the imidazole moiety in such scaffolds, we have decided to evaluate the effect of the π-extension of the imidazole ring on the electrochemical and photophysical properties and, in turn, on the ECL performance. In particular, we have selected the best performing compound among the series we have recently reported[13] and we substituted, as shown in Figure 1, the imidazole (Im) ring with benzimidazole (BenzIm) and with phenanthro[9,10-d]imidazole (PhenIm), respectively, while keeping the rest of the structure unchanged.

Results and Discussion

Synthetic Procedures

The imidazole derivatives 4$^{t\text{-}Bu}$CzBNIm and 4NPh$_2$BNIm have been already reported.[13] For the synthesis of the extended systems, as depicted in Scheme 1, we started from the commercially available 2,3,4,5,6-pentafluorobenzonitrile and selectively inserted the BenzIm or PhenIm at the *para* position in presence of a weak base such as caesium carbonate (in the case of PhenIm) or just in presence of an excess of 1H-benzo[d]imidazole for the BenzIm derivatives.[16] Then, through an aromatic nucleophilic substitution, we replaced all the remaining fluorine atoms with 3,6-di(*tert*-butyl)-9H-carbazole ($^{t\text{-}Bu}$Cz) or diphenylamine (NPh$_2$). Good yields were obtained for compounds 4$^{t\text{-}Bu}$CzBNBenzIm and 4$^{t\text{-}Bu}$CzBNPhenIm, while lower yields were obtained for compounds 4NPh$_2$BNBenzIm and 4NPh$_2$BNPhenIm (Scheme 1).

Interestingly, the restriction of the intramolecular rotation (RIR) due to the increasing π extension of the imidazole ring is already evident in solution in the ^{1}H NMR of the compounds bearing $^{t\text{-}Bu}$Cz. Indeed, the methyl groups of the t-BuCz groups become magnetically non-equivalent when carbazoles are restricted in their rotation around the bonding axis indicating a molecular stiffening due to the increased steric hindrance going from Im to BenzIm and PhenIm (Figure 2). Interestingly, while imidazole can be conveniently alkylated leading to a cationic and bioconjugable species,[13] our attempts to alkylate BenzIm and PhenIm derivatives failed.

Crystallographic Characterization

Single crystals, suitable for X-ray diffractometric analysis, were grown by slow diffusion of methanol or *n*-hexane vapours into chloroform.

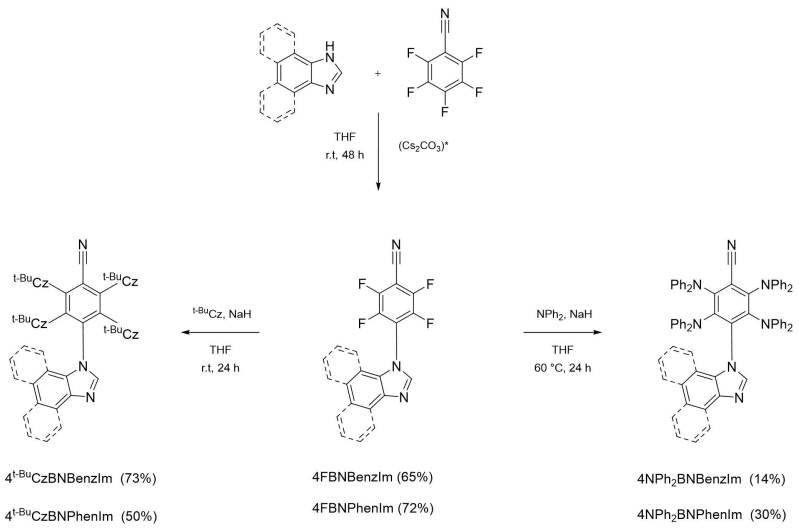

Scheme 1. Synthetic procedures for the imidazole precursor and final TADF compounds. (*) Cs_2CO_3 was used only for the synthesis of the PhenIm precursor.

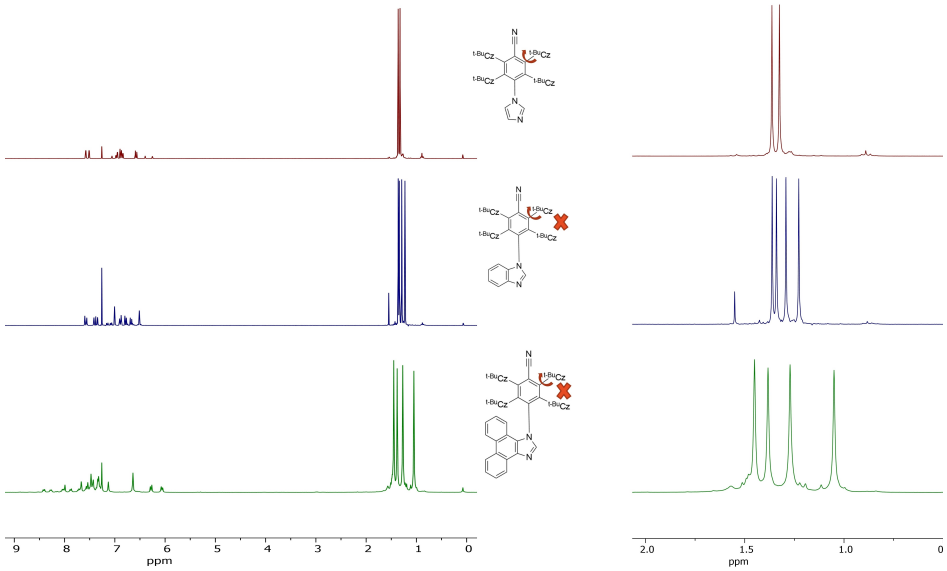

Figure 2. ^{1}H NMR spectra of 4$^{t\text{-Bu}}$CzBNIm (red), 4$^{t\text{-Bu}}$CzBNBenzIm (blue) and 4$^{t\text{-Bu}}$CzBNPhenIm (green).

The XRD structures of 4$^{t\text{-Bu}}$CzBNBenzIm, 4$^{t\text{-Bu}}$CzBNPhenIm and 4NPh$_2$BNPhenIm, shown in Figure 3, confirm the presence of the imidazole moiety in the *para* position and the substitution of all fluorine atoms with donors. As already known, the imidazole derivative fraction is almost perpendicular to benzonitrile,[13] so there should be a little orbital overlap that minimally affects the optoelectronic properties.

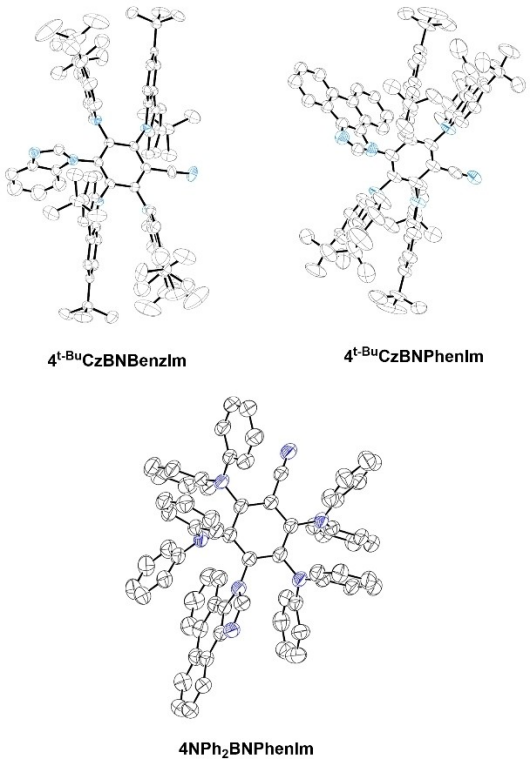

Figure 3. Ellipsoid representation of 4$^{t\text{-Bu}}$CzBNBenzIm, 4$^{t\text{-Bu}}$CzBNPhenIm and 4NPh$_2$BNPhenIm crystals (50% probability). Hydrogen atoms are omitted for clarity.

Electrochemical Characterization

The electrochemical properties of all compounds were studied by cyclic voltammetry both in anhydrous acetonitrile and anhydrous dichloromethane with a scan rate of 100 mVs^{-1}. All data are summarized in Table 1 and all the cyclovoltammograms are reported in Figures S1–S4.

In the cathodic region, a reversible peak ascribed to the benzonitrile acceptor is observed for all compounds, as already known in analogous systems,[12,13] while no electrochemical processes attributable to the imidazole moiety are observed. However, an anodic shift of the reduction process can be seen moving from Im to BenzIm and, more markedly, to PhenIm suggesting that the imidazole acts as an electron withdrawing group and increases the acceptor character of the benzonitrile.

The anodic region is characterized by multi-electronic oxidation processes. In particular, the carbazole derivatives display a higher reversibility in DCM rather than ACN while the diphenylamino derivatives seem more reversible than the 3,6-di(*tert*-butyl)carbazoyl congeners even if the pattern becomes more complex when moving to more extended imidazole rings, a molecular feature which seems not to improve the stability of the oxidized species. Overall, the voltammetric pattern in the anodic region is rather complex with the different diphenylamino or 3,6-di(*tert*-butyl)carbazoyl functions involved in multiple and, in many cases irreversible, electron transfers and a deep analysis of the details of the processes involved goes beyond the scope of this work. The observed signals in the anodic region are, in some cases, a convolution of multiple processes overlaid with

Table 1. Redox potentials of investigated compounds.

Compound	Acetonitrile solution		Dichloromethane solution	
	$E_{1/2}^{ox}$ (V)	$E_{1/2}^{red}$ (V)	$E_{1/2}^{ox}$ (V)	$E_{1/2}^{red}$ (V)
$4^{t\text{-}Bu}$CzBNIm	1.08;[a] 1.35[a]	−1.45	1.37	−1.58
$4^{t\text{-}Bu}$CzBNBenzIm	1.70[a]	−1.46	1.39; 1.66[a]	−1.54
$4^{t\text{-}Bu}$CzBNPhenIm	1.48;[a] 1.66[a]	−1.35	1.39; 1.52[a]	−1.39
$4NPh_2$BNIm	1.07; 1.32; 1.42[a]	−1.77	1; 1.2[a]	Not visible
$4NPh_2$BNBenzIm	0.78;[a] 1.12; 1.36	−1.76	0.81;[a] 1.05; 1.21	−1.80
$4NPh_2$BNPhenIm	0.79;[a] 1.06;[a] 1.17[a]	−1.67	1.10; 1.32; 1.62[a]	−1.72

Setup and conditions: WE: GCE (3 mm); RE: Ag/AgCl (sat. KCl) electrode (in agarose); CE: Pt wire. [Compound] = 1 mM. [$TBAPF_6$] = 0.1 M. Scan rate: 100 mVs^{-1}. [a] Irreversible peak, reported potential is peak potential.

the oxidation of possible products formed during the cathodic scan. For this reason, the oxidation potentials values reported in Table 1 cannot be safely used for thermodynamic considerations. Nonetheless, we can assert that the effect on the reduction potential of substituting the carbazole moieties with diphenylamine results, in both solvents, in a negative shift larger than 0.3 V. The diphenylamine then exerts a larger electro donating effect respect to carbazole inducing an energy increase in the molecule LUMO. Despite this, the HOMO-LUMO gap does not change significantly between the two series (this result is confirmed by computational studies in the following) meaning that the diphenylamine is more easily oxidized.

In order to evaluate the difference in the diffusive behaviour connected to the changes in the molecular structure of the imidazole moiety, the diffusion coefficient (*D*) values of the diphenylamino derivatives were calculated from the voltammetric peak currents values at different scan rate through the Randles–Ševčík equation[17] in DCM, the peak current is not always reliable for determining *D*; indeed, at slow scan rates, the peak assumes a sigmoidal shape typical of catalytic ECi processes, most likely due to the electron transfer from the electrogenerated radical anion and the solvent itself. However, by considering only the larger scan rates in DCM, reliable D data could be estimated for the NPh_2 series where *D* is observed to smoothly decrease with increasing molecular weight (from $9.1x10^{-6}$ cm^2s^{-1} for $4NPh_2$BNIm to $8.7x10^{-6}$ cm^2s^{-1} for $4NPh_2$BNBzIm and $4.5x10^{-6}$ cm^2s^{-1} for $4NPh_2$BNPheIm) and going from ACN and DCM in line with the expected differences in the solvent viscosity. These observations exclude the formation of supramolecular aggregates. From the *D* values, the molecular radius could be estimated by using the Stokes-Einsten equation, $D = k_BT/6\pi\eta r$, where k_B is the Boltzmann constant, η is the solvent viscosity, and *r* is the molecule radius. The *r* estimation in the two solvents was in good agreement and shows an increase going from Im to BenzIm and a more consistent change for $4NPh_2$BNPhenIm.

Photophysical Characterization

The photophysical properties of the synthesized compounds were investigated by recording the absorption, excitation and emission spectra and by determining the absolute photoluminescence quantum yields (PLQY) of the corresponding solutions in both anhydrous acetonitrile and anhydrous dichloromethane. In all UV-Vis absorption spectra it is possible to recognise characteristic transitions of D–A systems, which can be ascribed to internal charge transfer (ICT) in the 300–400 nm region.[18,19]

The absorption spectra are independent of the solvent polarity, as seen comparing Figure 4a with Figure S5, while the corresponding emission spectra show, as expected, a solvatochromic effect (see Figures 4b and S6). Indeed, for 3,6-di(*tert*-butyl)carbazoyl derivatives, there is a bathochromic shift of the emission maximum with increasing the polarity of the solvent, a typical behaviour in TADF emitters due to the CT nature of the electronic transition. The PLQYs follow the expected trend, i.e. decrease with increasing the solvent polarity. Moreover, they are highly sensitive to the presence of oxygen, suggesting that triplet excited states contribute to the PLQY. These observations are also further confirmed by the excited state lifetimes that shows the two typical components: the prompt fluorescence in the nanosecond timescale and the delayed emission in the microsecond range. Increasing the π-extension of the imidazole ring shifts to lower energy the absorption onset as well as bathochromically shifts the emission spectrum, as shown in Figure 4b (photoluminescence properties summarized in Table 2).

Surprisingly, a less trivial trend can be observed for compounds bearing diphenylamines as donors. Indeed, while a bathochromic shift of the absorption onset (Figure 4a) is observed going from BenzIm to PhenIm, as observed for the 3,6-di(*tert*-butyl)carbazoyl derivatives, the emission spectra are characterized by a hypsochromic shift and by higher PLQYs upon increasing solvent polarity. The latter are particularly evident in oxygen-free solutions. Time-resolved luminescence decay curves confirm the TADF nature also for the diphenylamine derivatives (Figures S11–S26).

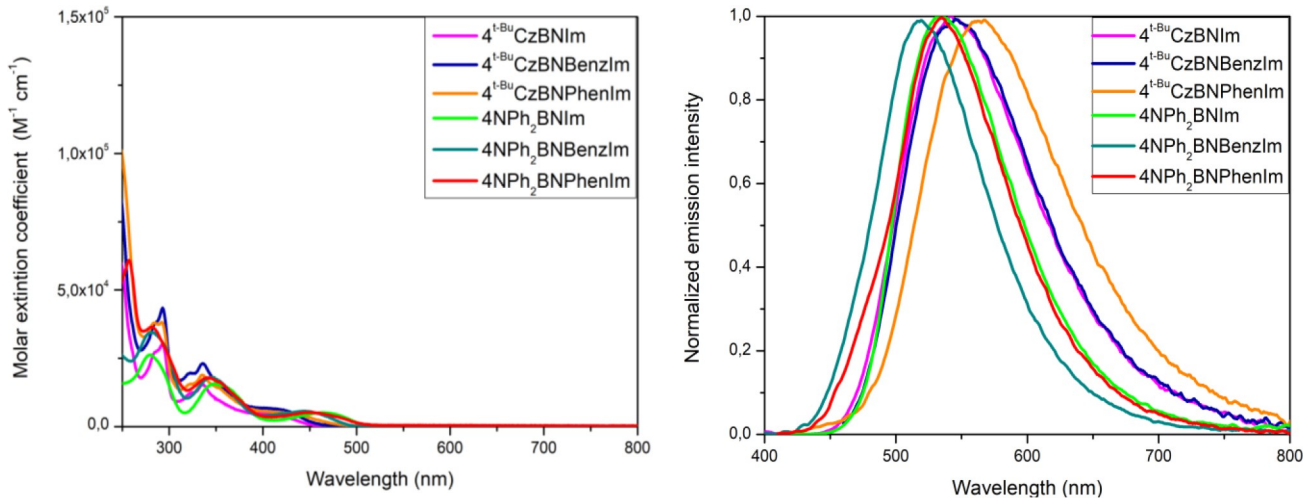

Figure 4. a) Absorption and b) normalized PL emission spectra of investigated compound in acetonitrile solution. Pink: $4^{t\text{-Bu}}$CzBNIm, blue: $4^{t\text{-Bu}}$CzBNBenzIm, yellow: $4^{t\text{-Bu}}$CzBNPhenIm, green: $4NPh_2$BNIm, cyan: $4NPh_2$BNBenzIm, red: $4NPh_2$BNPhenIm.

Table 2. Photoluminescent properties of investigated compounds in solution.

Compound	Solvent	λ_{max} (nm)[a]	τ_p (ns)[b]	τ_d (μs)[b]	Φ_{PL} (%)[c]	Φ_{PL} (%)[d]
$4^{t\text{-Bu}}$CzBNIm	DCM	525	15.4	1.444	28 ± 1	58 ± 2
	ACN	540	20.0	1.407	13.9 ± 0.8	22 ± 2
$4^{t\text{-Bu}}$CzBNBenzIm	DCM	532	11.3	1.735	25.5 ± 0.7	49 ± 1
	ACN	546	16.1	1.277	13.6 ± 0.5	20.5 ± 0.6
$4^{t\text{-Bu}}$CzBNPhenIm	DCM	552*	9.5	1.515	24.5 ± 0.5	31.4 ± 0.8
	ACN	564*	7.9	1.177	8.5 ± 0.4	10.6 ± 0.5
$4NPh_2$BNIm	DCM	532	2.3	10.41	7.7 ± 0.2	65 ± 2
	ACN	536	2.3	8.12	5.9 ± 0.2	9.8 ± 0.3
$4NPh_2$BNBenzIm	DCM	558	3.7	14.2	12 ± 3	29 ± 2
	ACN	518	2.9	5.9	8 ± 2	38 ± 2
$4NPh_2$BNPhenIm	DCM	573	4.1	44.2	9 ± 1	16 ± 1
	ACN	534	3.7	28.5	8.2 ± 0.9	27 ± 2

[Compound] = 5 μM, Φ_{PL} were evaluated using the absolute method, [a] λ_{exc} = 380 nm, * λ_{exc} = 420 nm. [b] Lifetimes were evaluated on Ar-purged solutions, λ_{exc} = 402.3 nm [c] Aerated solution; average scan λ_{exc} = 300–500 nm. [d] Ar-purged solution; average scan λ_{exc} = 300-500 nm.

Electrochemiluminescence

Electrochemiluminescence (ECL) analyses were performed under "reductive-oxidation" conditions using benzoyl peroxide (BPO) as coreactant. The mechanism consists in the application of a negative potential that leads to the generation of both the radical anion of the luminophore and the benzoate radical ($BO^{\bullet}$) ensuing from the O–O bond breaking of the reduced peroxide.[20] The latter behaves as a strong oxidant towards the radical anion of the emitter in solution, generating its excited species capable to relax through a radiative pathway, according to the following equations.

$$BPO + e^- \rightarrow BPO^{\bullet -}$$

$$BPO^{\bullet -} \rightarrow BO^{\bullet} + BO^-$$

$$LC + e^- \rightarrow LC^{\bullet -}$$

$$LC^{\bullet -} + BO^{\bullet} \rightarrow LC^* + BO^-$$

The choice of this particular analysis conditions stems from the electrochemical data of the luminophores here investigated, which reveal the presence of a reversible reduction process and irreversible/quasi-reversible multi-electron oxidation processes. As the benzoyl radical $BO^{\bullet}$ acts as an oxidizer in the electrochemical reaction generating the excited state, the luminophore oxidation potential must be lower than the standard potential of the $BO^{\bullet}/BO^-$ couple (+ 1.7 V vs NHE[21], ca. + 1.49 V vs Ag/AgCl[22]), which is the case for all investigated compounds as previously seen in Table 1.

The efficiency of the emitters was measured by chronoamperometry by applying a sequence of pulsed electrical

potentials (2 V, 0.3 Hz; Figure 5) and Φ_{ECL} were calculated by comparing the total ECL intensities with the total ECL intensity of the standard $[Ru(bpy)_3]Cl_2$ (for which ECL efficiency was assumed to be unitary) according to Equation (1).[10]

$$\Phi_{x,ECL} = \frac{\left(\frac{\int_a^b ECL\ dt}{\int_a^b i\ dt}\right)_x}{\left(\frac{\int_a^b ECL\ dt}{\int_a^b i\ dt}\right)_{St}} \quad (1)$$

Where x = sample, St = $[Ru(bpy)_3]Cl_2$.

The results are shown in Table 3.

Since the 3,6-di(*tert*-butyl)carbazoyl derivatives show higher photoluminescence quantum yields and better electrochemical features in DCM compared to ACN, as previously discussed, it is not surprising that the ECL efficiency mirrors this trend. However, an unexpected effect of the imidazole ring π extension on the ECL efficiency of the 3,6-di(*tert*-butyl)carbazoyl derivatives is observed in DCM with Φ_{ECL} BenzIm > Im ≫ PhenIm while in ACN the ECL efficiency mirrors the PLQY efficiencies with Im > BenzIm > PhenIm. For the diphenylamine derivatives, irrespective to our expectations, increasing the extension of the imidazole ring has a negative impact on the ECL efficiency that significantly drops going from Im to PhenIm, even in ACN where the PLQYs display the opposite trend.

The observed trend in ECL efficiency using BPO as a coreactant is also maintained under annihilation conditions and with TPA as a coreactant (Tables 4 and 5, Figures S37–

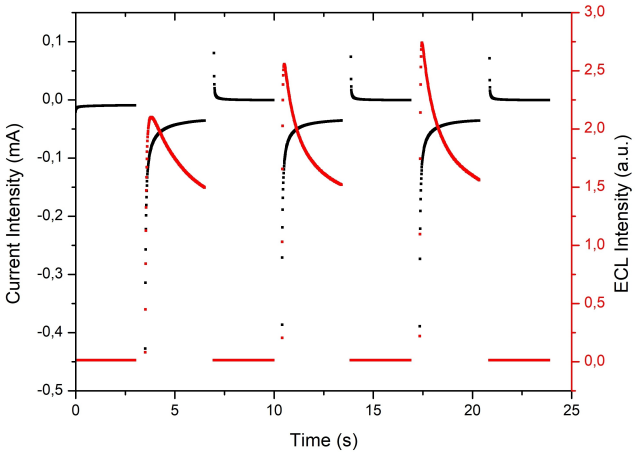

Figure 5. Coreactant ECL–time (red) and current–time (black) profiles of $4^{t\text{-}Bu}$CzBNBenzIm in dichloromethane.

Table 3. ECL properties of investigated compounds in solution with BPO as coreactant.

Compound	Solvent	λ_{ECL} (nm)	Φ_{ECL} [a]
$4^{t\text{-}Bu}$CzBNIm	DCM	529	11 ± 3
	ACN	545	4.7 ± 0.6
$4^{t\text{-}Bu}$CzBNBenzIm	DCM	537	20 ± 3
	ACN	545	2.3 ± 0.4
$4^{t\text{-}Bu}$CzBNPhenIm	DCM	556	3.0 ± 0.4
	ACN	563	1.4 ± 0.5
$4NPh_2$BNIm	DCM	533	28 ± 4
	ACN	528	12 ± 2
$4NPh_2$BNBenzIm	DCM	536	9 ± 2
	ACN	529	3.2 ± 0.6
$4NPh_2$BNPhenIm	DCM	552	5.5 ± 1.4
	ACN	549	0.9 ± 0.2

Setup and conditions: WE: GCE (3 mm); RE: Ag/AgCl (sat.d KCl) electrode (in agarose); CE: Pt wire. [Compound] = 50 μM; [BPO] = 1 mM; $[TBAPF_6]$ = 0.1 M. Potential sequence (repeated three times): 0 V for 3 s, −2 V for 3 s, 0 V for 3 s. All experiments were performed three times each. [a] Calculated from Equation (1) assuming the ECL efficiency of $[Ru(bpy)_3]Cl_2$ = 1.

Table 4. ECL properties of investigated compounds in acetonitrile solution with TPA as coreactant.

Compound	λ_{ECL} (nm)	Φ_{ECL} [a]
$4^{t\text{-}Bu}$CzBNIm	529	0.39
$4^{t\text{-}Bu}$CzBNBenzIm	548	0.27
$4^{t\text{-}Bu}$CzBNPhenIm	569	0.03
$4NPh_2$BNIm	533	1.4
$4NPh_2$BNBenzIm	537	0.05
$4NPh_2$BNPhenIm	546	0.06

Setup and conditions: WE: GCE (3 mm); RE: Ag/AgCl (sat.d KCl) electrode (in agarose); CE: Pt wire. [Compound] = 50 μM; [TPA] = 1 mM; $[TBAPF_6]$ = 0.1 M. Potential sequence (repeated three times): 0 V for 3 s, +1.5 V for 3 s, 0 V for 3 s. [a] Calculated from Equation (1) assuming the ECL efficiency of $[Ru(bpy)_3]Cl_2$ = 1.

Table 5. ECL properties of investigated compounds in acetonitrile solution under annihilation conditions.

Compound	Applied potentials	Φ_{ECL} [a]
$[Ru(bpy)_3]Cl_2$	−1.5 V and +1.5 V	1
	+1.5 V and −1.5 V	1
$4^{t\text{-}Bu}$CzBNIm	−1.7 V and +1.3 V	1.4 ± 0.9
	+1.3 V and −1.7 V	0.27 ± 0.09
$4^{t\text{-}Bu}$CzBNBenzIm	−1.6 V and +1.5 V	0.58 ± 0.08
	+1.5 V and −1.6 V	0.56 ± 0.13
$4^{t\text{-}Bu}$CzBNPhenIm	−1.5 V and +1.6 V	0.12 ± 0.04
	+1.6 V and −1.5 V	0.35 ± 0.14
$4NPh_2$BNIm	−2 V and +1.3 V	38 ± 6
	+1.3 V and −2 V	12 ± 4
$4NPh_2$BNBenzIm	−2 V and +1 V	0.03 ± 0.01
	+1 V and −2 V	0.03 ± 0.02
	−2 V and +1.2 V	0.07 ± 0.02
	+1.2 V and −2 V	0.04 ± 0.02
$4NPh_2$BNPhenIm	−2 V and +1 V	0.07 ± 0.02
	+1 V and −2 V	0.05 ± 0.01
	−2 V and +1.2 V	0.14 ± 0.02
	+1.2 V to −2 V	0.16 ± 0.03

Setup and conditions: WE: GCE (3 mm); RE: Ag/AgCl (sat.d KCl) electrode (in agarose); CE: Pt wire. [Compound] = 20 μM; $[TBAPF_6]$ = 0.1 M. Potential were stepped with a frequency of 10 Hz and their values are reported near the respective compound. [a] Calculated from Equation (1) assuming the ECL efficiency of $[Ru(bpy)_3]Cl_2$ = 1.

S42, S47 and S48). In all cases the imidazole derivatives show higher efficiencies than their more extensively conjugated counterparts.

Moreover, annihilation experiments have also shown that for the diphenylamino derivatives (Figures S39 and S40), independently from the imidazole extension, light emission is only observed when we first generate the radical anion and secondly the radical cation and not vice versa suggesting that the radical cation has a shorter lifetime in solution with respect to the radical anion. In addition, an increase of 200 mV in the oxidation potential increases the emission intensity at the expanses of the stability (Figures S41 and S42). Interestingly, in the case of $^{t\text{-Bu}}$Cz derivatives, the stability of the generated radical species seems to be more affected by the extension of the imidazole. Indeed, while in 4$^{t\text{-Bu}}$CzBNBenzIm the light emission seems to be independent by the pulse sequence, in 4$^{t\text{-Bu}}$CzBNPhenIm we observed the opposite behaviour, i.e. light is emitted only when we first generate the radical cation and secondly the radical anion. These results suggest that the extension of the imidazole moieties has a detrimental effect on the stability of the radical anion.

Based on these data, several hypotheses could be considered to explain the unexpected results. First, the reduced diffusion due to the larger size of the molecule involved contributes to slowing down the formation of the excited chromophore. Second, as an electron transfer reaction is observed between the electrogenerated radical anions and the DCM, this could also be feasible for the excited state. A photocatalytic reaction involving the DCM could contribute to making the light emission less efficient therefore to an apparent increase of PLQY in ACN.

DFT Analysis

Full geometry optimizations were carried out on six compounds, to investigate the structural and electronic variations upon replacing Im with BenzIm and PhenIm, as well as when replacing Cz with NPh_2 (level of theory: ZORA-BLYP-D3(BJ)/TZ2P.[23,24] In the models, the *tert*-butyl groups of the Cz ligands were changed to H. The optimized structures are shown in Figure S60. When increasing the size of the imidazole moiety, it progressively moves toward an orthogonal arrangement with respect to the central aromatic core, both for Cz and for NPh_2 derivatives. In particular, 4NPh_2BNPhenIm displays the most orthogonal arrangement (close to 90°), likely stabilized by stacking interactions with the phenyls of the amine ligands (the distance between the centre of the amino phenyls and the central phenyl moiety of phenanthrene is ~3.5 Å). As already described in the literature,[1,25] the HOMO of the Cz derivatives is mainly ligand centred, while the LUMO has anti bonding lobes on the benzonitrile core (Figure S61). A similar picture emerges for the NPh_2 compounds, i.e., the HOMO is centred on the amino ligands, but exhibits large lobes also on the central BN core too, while the LUMO has anti bonding character and is centred on the benzonitrile moiety, as shown in Figure 6 for 4NPh_2BNBenzIm. The HOMO-LUMO gaps are shown in Table S2. Both Cz and NPh_2 series show the same trend, i.e., the gap decreases when going from Im to PhenIm and is larger in the former series than in the latter. The nature of the frontier orbitals and their energy separation anticipate the presence of CT absorption in the visible region, which was confirmed by computing the lowest excitations and their oscillator strength (level of theory: COSMO-ZORA-TD-B3LYP/TZP ae). In this set of calculations, solvation was included using a continuum model to approximate the effect of media of different polarity. The results are shown in Table 6 where the lowest excitations, their oscillator strength and character are listed for the NPh_2 compounds.

The CT nature of the lowest absorption is confirmed (Figure 6). We observe a systematic bathochromic shift with increasing solvent polarity as well when moving from Im to BenzIm, in nice agreement with the experiment. This enhanced our confidence in the adequacy of the employed methodology to study excited state properties of these systems. Thus, in the attempt of rationalizing the experimentally observed hypsochromic shifts in the emission spectra, we explored the hypothesis that strong modifications may occur in the excited state, i.e., a different mutual orientation of the ancillary ligand and the benzonitrile moiety compared to the ground state. A scan was performed on 4NPh_2BNIm and 4NPh_2BNBenzIm in both solvents and the excited state profile was built using time-dependent single point calculations. The energy profiles of the ground (S_0) and lowest excited state (S_1) are shown in Figure S63. We observe that for the Im derivatives, in both solvents, the minimum energy

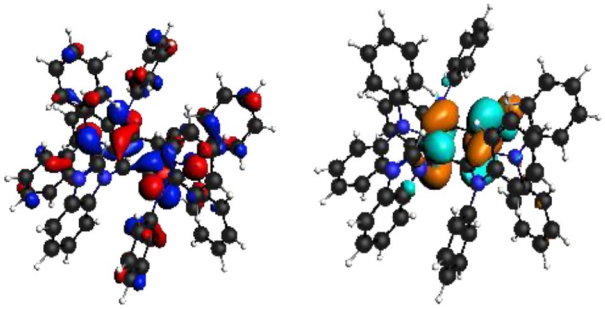

Figure 6. Kohn-Sham frontier molecular orbitals of 4NPh_2BNBenzIm: HOMO (left) and LUMO (right). Level of theory: ZORA-BLYP-D3(BJ)/TZ2P. Isodensity: 0.02.

Table 6. Computed lowest excitation energies (eV), oscillator strength, assignments. Level of theory: COSMO-ZORA-TD-B3LYP/TZP ae.

Compound	Solvent	exc (eV)	f	Assignment
4NPh_2BNIm	DCM	2.3462	0.21881	H→L (98.7%)
	ACN	2.3246	0.23624	H→L (98.7%)
4NPh_2BNBenzIm	DCM	2.3050	0.19940	H→L (98.7%)
	ACN	2.2875	0.21516	H→L (98.7%)
4NPh_2BNPhenIm	DCM	2.2873	0.20406	H→L (98.5%)
	ACN	2.2689	0.22128	H→L (98.5%)

conformation computed in the gas-phase is maintained and rotation is not sterically hindered. The lowest excited state energy profile matches to the ground state profile and is merely shifted. For the BenzIm species, along the rotation, a local minimum appears in correspondence of a 120° tilted arrangement of the benzonitrile and BenzIm moieties. However, no significant geometry differences are predicted between the ground and the lowest excited state.

Conclusions

In this work, a new class of imidazole derivatives with thermally activated delayed fluorescence (TADF) properties were synthesized and structurally characterized. Maintaining the same scaffold, we investigated the effect of the different π-extension of the imidazole moiety on the photophysical, electrochemical and electrochemiluminescence properties. Interestingly we have found that increasing the π-extension of the imidazole moiety leads to a restriction of the intramolecular rotation (RIR) in solution as observed in ^{1}H NMR analysis and it also results in a bathochromic shift of both absorption and emission spectra. DFT analysis revealed that the HOMO-LUMO energy gap decreases going from the Im to BenzIm and PhenIm. Unfortunately, the RIR effect observed in solution do not improve the PLQY that decreases significantly together with the ECL efficiency. Surprisingly, the effect of RIR that should lead to higher PLQY and hypsochromic shift of the emission is observed only in the *NPh$_2$* derivatives when the solvent polarity is increased. We believe that, in the analysed series, the absolute value of the LUMO orbital could be relevant, in particular in DCM, where the strong reducing character of the excited fluorophores could trigger competing non-radiative reaction paths. Even if unexpected, our results could contribute to open new strategies towards the development of bright TADF emitters in highly polar media.

Supporting Information

Experimental procedures, cyclic voltammetries, UV-vis absorption, emission and excitation spectra, lifetimes decays, ECL-voltage curves, ECL spectra, ECL and chronoamperometric profiles and crystallographic information are provided in the Supporting Information. Deposition Numbers 2322130 (for 4$^{t\text{-Bu}}$CzBNBenzIm), 2322129 (for 4$^{t\text{-Bu}}$CzBNPhenIm) and 2284116 (for 4NPh$_2$BNPhenIm) contain the supplementary crystallographic data for this paper. These data are provided free of charge by the joint Cambridge Crystallographic Data Centre and Fach informations zentrum Karlsruhe Access Structures service.

Acknowledgements

The authors are grateful to the financial support from MIUR under the FARE framework (R20S3XECXT) and PRIN PNRR 2022 SupraPhotoChem (P2022WLAY7). Emission spectra, excitation spectra and lifetime decay measurements were performed on an Edinburgh FLS 1000 UV/Vis/NIR photoluminescence spectrometer at the PanLab department facility, founded by the MIUR- "Dipartimenti di Eccellenza" grant NExuS. Dr. Ilaria Fortunati is acknowledged for her assistance in emission spectra, excitation spectra and lifetime decay measurements. Dr. Marco Roverso and Prof. Sara Bogialli are acknowledged for HRMS experiments. CNAF (https://www.cnaf.infn.it/) is acknowledged for the generous allocation of computational resources. Open Access publishing facilitated by Università degli Studi di Padova, as part of the Wiley - CRUI-CARE agreement.

Conflict of Interests

The authors declare no conflict of interest.

Data Availability Statement

The data that support the findings of this study are available from the corresponding author upon reasonable request.

Keywords: thermally activated delayed fluorescence · electrochemiluminescence · imidazole derivatives · luminescence

[1] H. Uoyama, K. Goushi, K. Shizu, H. Nomura, C. Adachi, *Nature* **2012**, *492*, 234–238.
[2] W. Li, Y. Pan, R. Xiao, Q. Peng, S. Zhang, D. Ma, F. Li, F. Shen, Y. Wang, B. Yang, Y. Ma, *Adv. Funct. Mater.* **2014**, *24*, 10.1002/adfm.201301750.
[3] M. A. Bryden, E. Zysman-Colman, *Chem. Soc. Rev.* **2021**, *50*, 10.1039/d1cs00198a.
[4] R. Ishimatsu, S. Matsunami, T. Kasahara, J. Mizuno, T. Edura, C. Adachi, K. Nakano, T. Imato, *Angew. Chem., Int. Ed.* **2014**, *53*, 6993–6996.
[5] Y. Tao, K. Yuan, T. Chen, P. Xu, H. Li, R. Chen, C. Zheng, L. Zhang, W. Huang, *Adv. Mater.* **2014**, *26*, 7931–7958.
[6] P. De Silva, C. A. Kim, T. Zhu, T. Van Voorhis, *Chem. Mater.* **2019**, *31*, 6995–7006.
[7] X. K. Chen, D. Kim, J. L. Brédas, *Acc. Chem. Res.* **2018**, *51*, 2215–2224.
[8] P. Huang, X. Zou, Z. Xu, Y. Lan, L. Chen, B. Zhang, L. Niu, *Molecules* **2022**, *27*, 7457.
[9] J. Ludvík, *J. Solid State Electrochem.* **2011**, *15*, 2065–2081.
[10] M. M. Richter, *Chem. Rev.* **2004**, *104*, 3003–3036.
[11] H. Al-Kutubi, S. Voci, L. Rassaei, N. Sojic, K. Mathwig, *Chem. Sci.* **2018**, *9*, 8946–8950.
[12] E. Speckmeier, T. G. Fischer, K. Zeitler, *J. Am. Chem. Soc.* **2018**, *140*, 15353–15365.
[13] G. Pavan, L. Morgan, N. Demitri, C. Alberoni, T. Scattolin, A. Aliprandi, *Chem. – Eur. J.* **2023**, e202301912, 10.1002/chem.202301912.
[14] Z. Yang, Z. Mao, Z. Xie, Y. Zhang, S. Liu, J. Zhao, J. Xu, Z. Chi, M. P. Aldred, *Chem. Soc. Rev.* **2017**, *46*, 915–1016.
[15] J. Mei, Y. Hong, J. W. Y. Lam, A. Qin, Y. Tang, B. Z. Tang, *Adv. Mater.* **2014**, *26*, 5429–5479.
[16] H. I. Althagbi, J. R. Lane, G. C. Saunders, S. J. Webb, *J. Fluorine Chem.* **2014**, *166*, 88–95.
[17] A. J. Bard, L. R. Faulkner, *Electrochemical Methods, Fundamentals and Applications*, Wiley, New York **2001**.
[18] R. Ishimatsu, T. Edura, C. Adachi, K. Nakano, T. Imato, *Chem. - Eur. J.* **2016**, *22*, 4889–4898.
[19] Q. Zhang, J. Li, K. Shizu, S. Huang, S. Hirata, H. Miyazaki, C. Adachi, *J. Am. Chem. Soc.* **2012**, *134*, 14706–14709.

[20] K. M. Omer, S. Y. Ku, Y. C. Chen, K. T. Wong, A. J. Bard, *J. Am. Chem. Soc.* **2010**, *132*, 10944–10952.
[21] W. Miao, *Chem. Rev.* **2008**, *108*, 2506–2553.
[22] V. V. Pavlishchuk, A. W. Addison, *Inorg. Chim. Acta* **2000**, *298*, 97–102.
[23] M. Bortoli, F. Zaccaria, M. D. Tiezza, M. Bruschi, C. F. Guerra, F. Matthias Bickelhaupt, L. Orian, *Phys. Chem. Chem. Phys.* **2018**, *20*, 20874–20885.
[24] A. Madabeni, M. Dalla Tiezza, F. B. Omage, P. A. Nogara, M. Bortoli, J. B. T. Rocha, L. Orian, *J. Comput. Chem.* **2020**, *41*, 2045–2054.
[25] J. H. Kim, J. H. Yun, J. Y. Lee, *Adv. Opt. Mater.* **2018**, *6*, 1800255.

Manuscript received: March 27, 2024
Revised manuscript received: June 25, 2024
Accepted manuscript online: July 22, 2024
Version of record online: ■■, ■■

ACES Asian Chemical Editorial Society

CHEMISTRY
AN ASIAN JOURNAL
Research Article

RESEARCH ARTICLE

We investigate the impact of the π-extension of the imidazole moiety in a series of thermally activated delayed fluorescence emitters on their electrochemical photophysical end electrochemiluminescence properties. A restriction of the intramolecular rotation (RIR) has been observed in solution as the π-extension is increased, however the smallest perform better.

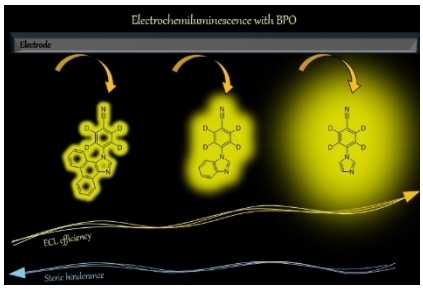

*E. Pelorosso, G. Pavan, T. Scattolin, L. Orian, S. Antonello, N. Demitri, A. Aliprandi**

1 – 10

Effect of the Imidazole π-Extension on TADF Emitters in Electrochemiluminescence